

COMPARISON OF NUMERICAL AND EXPERIMENTAL SPEEDS AND FLOW MASS ON EXIT OF THE TEST SECTION OF A LOW SPEED WIND TUNNEL.

Soares, Cleide Barbosa cleide_bsoares@hotmail.com

Federal Center of Technological Education of Minas Gerais-CEFET-MG, Av. Amazonas, 5.253 – Nova Suíça - Belo Horizonte, Minas Gerais, Brazil- Cep. 30480-000

Hanriot, Sérgio de Moraes, hanriot@pucminas.br

Maia, Cristiana Brasil, cristiana@pucminas.br

Cabezas-Gómez, Luben, luben@pucminas.br

Guzella, Matheus dos Santos, matheusguzella@gmail.com

Ledo, Luiz Fernando Ribeiro, lribeiroledo@yahoo.com.br

Pontifical Catholic University of Minas Gerais-PUC-MG, Av. Dom José Gaspar, 500 – Coração Eucarístico - Belo Horizonte, Minas Gerais, Brazil – Cep. 30535-610

Abstract. Aerodynamic studies seek primarily the maintenance, at the examined bodies, of the named dynamic equilibrium state. In order to run aerodynamics experiments, most of research laboratories use wind tunnels to analyze the air streamlines around bodies. Tests performed in wind tunnels offer the possibility to determine the intensity of the acting forces to obtain the result of its three components: lift forces, resistance to displacement of the model and forces associated with side loads. It is worth to notice the interest in visualize the streamlines of air, during testing of the model in a wind tunnel. This paper presents numerical and experimental results of an open low-speed wind tunnel with total length of 2990 mm. The tunnel is composed of six parts: diffuser section circular to square, two large diffusers angle, stagnation section, contraction and square test section of 790 mm in length and 200 mm wide. The experimental tests were conducted in the exit region of the tunnel test section using a Pitot tube and a hot wire anemometer. The numerical predictions were performed by solving the Reynolds-Averaged Navier–Stokes (RANS) equations using the Shear Stress Transport (SST) $k-\omega$ turbulence model with the ANSYS-CFX® code. A numerical solution of a fully developed turbulent channel flow is also presented for comparison purpose. The numerical values of axial velocity were compared with the measurements in the exit region of the tunnel. The turbulent kinetic energy was compared in the central point of the exit cross-section of the tunnel. The results are in good agreement with the experimental data.

Keywords: CFD, wind tunnel, SST $k-\omega$ turbulence model, Pitot tube, Hot Wire Anemometry.

1. INTRODUCTION

Wind tunnels are equipments designed to help the study of the effect of fluids around bodies. Air is blown through a duct, in which geometrical forms (such as automobiles or aircraft wings) are positioned. According to Baker (2007), although the first wind tunnel predated the advent of airplanes, with Wenham in 1871, the development of the wind tunnel was driven by the aeronautical industry in the period 1900 to 1960, when it was seen primarily as a research tool. Between 1960 and 1980, it developed to a reliable and robust tool for industrial and commercial design purposes.

According to Metha and Bradshaw (1979), it is not easy to establish design rules for wind tunnels, due to the variety of needs and configurations of components in a wind tunnel. However, Winkler et al (2007) suggests that an optimal design of a wind tunnel should prioritize building flexible modules, allowing easy and quick release if needed. The load losses must be properly calculated for installation and blower specification and design of the tunnel should allow the implementation of additional screens that can be removed or exchanged.

In a test section of wind tunnel the airflow must meet high standards to provide the data collection as well as accurate and reliable results, because high demands are motivated by the large number of studies conducted in wind tunnels and their importance (Moonen et. al, 2007).

Today, General Motors (GM) has one of the largest wind tunnels, applied to the automotive industry in real scale. This tunnel is equipped with a closed-loop system, whose function is to assess the aerodynamic performance, directional stability and thermal comfort in passenger cars and medium-sized enterprises (Quim, 2007). There are proposals for wind tunnels that help aircraft design, however these projects are complicated besides this they require high costs. To solve this problem a numerical wind tunnel was created, as described by Kim et.al (2006).

Carregari (2006) used the wind tunnel installed in the premises of the School of Engineering of São Carlos (EESC), at the Aeronautical Research Center (NPA) in the Aerodynamics Laboratory (LAE), to analyze the behavior of the flow around a scale model of a bus.

Liu et al. (2008) studied mean drag and lift coefficients for groups of two, three, and four cylinders arranged in-line. Drag and lift forces were measured in smooth and turbulent flow conditions. Liu et. al (2010) studied the air pollutant dispersion characteristics under different normal wind directions. A typical high-rise residential building design in Hong

Kong was investigated in a wind tunnel design. Several other studies were performed using wind tunnels: study of the development of secondary instabilities in compressible swept airfoil boundary layers, study on exhaust gas dispersion from road vehicles (Kandaa et al., 2006,a Kandaa et al., 2006,b) and the evaluation of the effect of long-term flights in birds (Jenni-Eiermann et al., 2009).

This paper presents a comparison between the numerical and experimental results of velocity, flow rate and turbulent kinetic energy in a low-speed wind tunnel. The numerical results obtained through computer simulations using the commercial software ANSYS CFX were validated with experimental data obtained in a prototype, using the techniques of Pitometry and hot wire thermal anemometry (HWA) at constant temperature.

2. METHODOLOGY

2.1 Numerical Methodology

A CFD technique comprehends the numerical solution of the governing flow equations and boundary conditions. In the analysis, the solution domain is divided into a large number of infinitesimal control volumes and the governing equations are solved for each of them. The main governing equations of fluid flow are mass conservation, momentum conservation. The effects of turbulence are considered through the application of the $k-\omega$ SST turbulence model. A previous study (Queiroz et.al 2009), showed better behavior and adaptations of the simulation model of turbulent kinetic energy.

The mass conservation and momentum conservation equations are used in the same form for all the models evaluated.

Mass conservation:

$$\frac{\partial \rho}{\partial t} + \vec{\nabla} \cdot (\rho U) = 0 \quad (1)$$

Where ρ represents the specific mass of the fluid and U is the velocity vector.

Momentum conservation:

$$\frac{\partial(\rho U)}{\partial t} + \vec{\nabla} \cdot (\rho U \otimes U) - \vec{\nabla} \cdot (\mu_{eff} \vec{\nabla} U) = -\vec{\nabla} p' + \vec{\nabla} (\mu_{eff} (\vec{\nabla} U))^T + B \quad (2)$$

Where U stands for the mean velocity vector, ρ represents the density of the fluid, B is the sum of body forces, μ_{eff} is the effective viscosity accounting for turbulence, and p' is the modified pressure. μ_{eff} and p' are given respectively by:

$$\mu_{eff} = \mu + \mu_t \quad (3)$$

$$p' = p + \frac{2}{3} \rho k \quad (4)$$

The eddy viscosity ν_t is:

$$\nu_t = \frac{a_1 k}{\max(a_1 w, SF_2)} \quad (5)$$

Where S represents an invariant measure of the strain rate. F_2 is a blending function, which restricts the limiter to the wall boundary layer.

The constants used in the SST model equations are the standard (Malalasekera; Versteeg, 1995).

The turbulent kinetic energy, k and turbulent frequency, ω are computed by the following relation, Eq. (6) and (7), respectively:

$$\frac{\partial(\rho k)}{\partial t} + \vec{\nabla} \cdot (\rho U k) = \vec{\nabla} \cdot \left[\left(\mu + \frac{\mu_t}{\sigma_{k3}} \right) \vec{\nabla} k \right] + P_k - \beta' \rho k \omega \quad (6)$$

$$\frac{\partial(\rho\omega)}{\partial t} + \vec{\nabla} \cdot (\rho U \omega) = \vec{\nabla} \cdot \left[\left(\mu + \frac{\mu_t}{\sigma_{\omega 3}} \right) \vec{\nabla} \omega \right] + (1 - F_2) 2\rho \frac{1}{\sigma_{\omega 2} \omega} \vec{\nabla} k \vec{\nabla} \omega + \alpha_3 \frac{\omega}{k} P_k - \beta_3 \rho \omega^2 \quad (7)$$

The numerical simulations of airflow in the tunnel section tests were performed considering the rotation speed of 3000 rpm with a screen and no screen between diffusers, corresponding to mass flow rates of 0.31 m³/s and 0.32 m³/s respectively.

The solution domain included the test section of the wind tunnel. The geometric parameters are the same of the experimental prototype, a square section of 200 mm x 200 mm and length of 790 mm.

The hypotheses considered on the analysis were: air as an ideal gas, heat transfer model isothermal (the ambient temperature was defined as 288.15K). The atmospheric pressure was considered as 90.6kPa. Both values were measured in the experiments steady state conditions and buoyancy effects were not considered.

The flow direction was established as normal to the boundary condition and conditions of medium intensity and eddy viscosity ratio turbulence were imposed. At the walls, it was assumed the no slip boundary condition, meaning that the fluid velocity at the walls has a zero value. At the outlet, it was assumed a subsonic flow with an average static pressure, over the entire outlet region, equal to zero.

2.1.2 Correlations for pressure drop and boundary layer thickness computation

The numerical pressure drop along the test section is compared with a pressure drop computed for a turbulent developed flow using a traditional procedure. The pressure drop in this case is calculated by Eq. (8):

$$\Delta_p = f \frac{\rho u_m^2 L}{2D_h} \quad (8)$$

Where f is the friction factor considering a smooth duct.

The Reynolds number is computed as:

$$\text{Re}_{D_h} = \frac{\rho u_m D_h}{\mu} \quad (9)$$

The boundary layer thickness of the turbulent flow inside the test section was computed as in Eq. (10), considering the correlation for an external flow over a flat plate:

$$\frac{\delta}{z} = 0,37 \text{Re}_z^{-0,2} \quad (10)$$

Where Re_z is given by:

$$\text{Re}_z = \frac{\rho u_m z}{\mu} \quad (11)$$

2.2 Experimental setup

Experimental measurements were carried out in the open low speed wind tunnel, of total length of 2990 mm. The following parts compose it: circular cross-section to square cross-section diffuser, wide-angle diffusers, stagnation section, contraction section and test section of 790 mm. Diffusers, location of the screens, blowers and flow direction are shown in Figure 1.

The wind tunnel was originally fitted with screens between broadcasters and subsequently no screens between diffusers, for tests with the Pitot tube and hot wire anemometer and a constant temperature (HWA).

Afterwards with these pressure values were determined the local velocity values in each measurement point, and the mean velocity and volumetric flow rate in the entire section. Reference to the experimental procedures was conducted in accordance with recommendations of the ISO 3966 (2008).

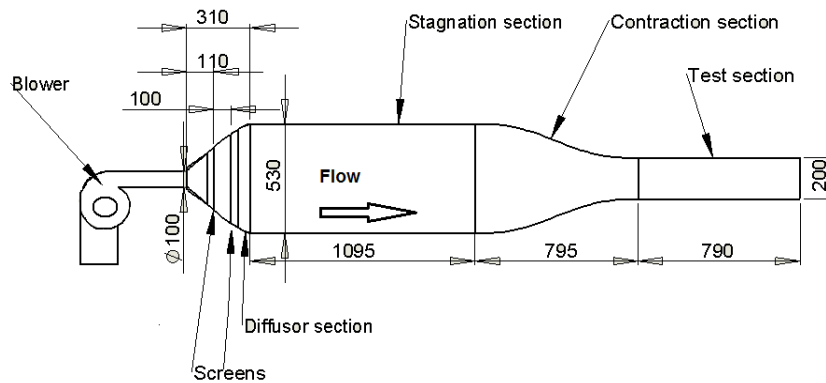
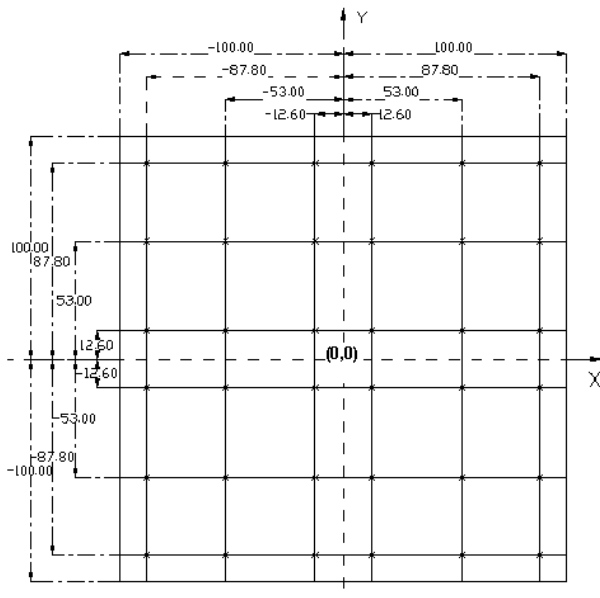


Figure 1: Schematics of the wind tunnel

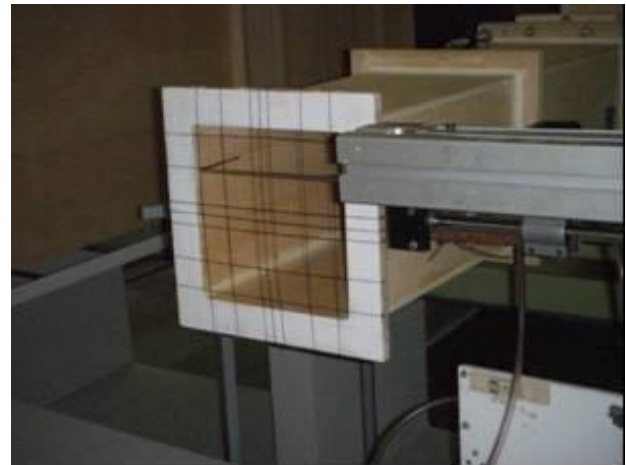
The International Organization for Standardization Division standardizes the output of the cross section of duct test section that was divided into 36 points by Log-Chebyshev (ISO 3966, 2008), Fig 2 A. The blower was driven at 15 frequencies ranging from 1800 to 3200 rpm with an increment of 100 rpm. The Pitot tube was positioned at the intersection of X and Y coordinates as shown in Figure 2 (A) and 2 (B).

The ASTM International normalizes and recommends testing procedures with the hot wire anemometer at constant temperature (ASTM D 3464, 2007). A hot wire anemometer was placed in the centre of the test section (0,0 coordinates) to evaluate the instantaneous velocity and the intensity of turbulence of the airflow at this point. In the experiments, the room temperature was 294 K and the atmospheric pressure was 0.906 bar.

For the tests with hot wire anemometry constant temperature (HWA), it was used a probe with one sensor element, reference code-Dantec 55P11, capable of measuring only one component of the velocity vector and its fluctuations. Its characteristics are: length 1.25 mm and diameter of 5 μ m.



2(A)



2(B)

Figure 2(A) e 2 (B): Velocity Measurement Points and Pitot tube and test section

2.3 Uncertainty Analysis

The uncertainty is a parameter, associated with the result of a measurement, which characterizes the dispersion of values that can be reasonable, attributed to the variable (ISO 3966:2008). The combined standard uncertainty, associated with a measurement of local velocity, v , is obtained by combining the standard deviations of errors arising from the sources present in Eq. (12). The combination of the random and systematic errors may therefore be treated as

though all were truly random, and the standard deviation for the systematic components can be obtained by calculating a value for their standard deviations. The coefficient of variation of the local velocity measurement is then the square root of the sum of the squares of the coefficients of variation arising from the sources of errors. Thus the result of the local velocity measurement is:

$$v = \left\{ 1 \pm 2 \left[\frac{1}{4} \left(\frac{\sigma \Delta p}{\Delta p} \right)^2 + \left(\frac{\sigma f}{v} \right)^2 + \left(\frac{\sigma p}{\rho} \right)^2 + \left(\frac{\sigma c}{v} \right)^2 + \left(\frac{\sigma t}{v} \right)^2 + \left(\frac{\sigma g}{v} \right)^2 + \left(\frac{\sigma \phi}{v} \right)^2 \right]^{\frac{1}{2}} \right\} \quad (12)$$

Where:

- v = Local velocity of the fluid.
- Δp=Differential pressure measured by the Pitot tube.
- σf=Velocity of fluctuation
- σg=Density of fluid
- σc=Pitot tube calibration
- σt=Turbulence
- σg=velocity gradient
- σφ=Pitot tube inclination

3. RESULTS AND DISCUSSIONS

The numerical and experimental results are presented of 3000 rpm blower.

3.1 Numerical results

The numerical simulations were obtained using the software ANSYS-CFX® 11.0 on a Intel (R) Core(TM) i5 CPU 750 @ 2.67 GHz - 4.00GB RAM. According to ANSYSCFX® (2009), tetrahedral elements are not efficient for capturing boundary layers effects, and then prismatic elements near the walls needs to be constructed. In the present work were created three unstructured hybrid meshes (mesh 1, 2 and 3 respectively), using the software ANSYS ICEM CFD® 12.1, with tetrahedral elements, in the central regions and prismatic elements near the tunnel walls, in order to capture boundary layers features (Fig. 3). The computational meshes were constructed considering an increasing number of nodes.

Table 1 shows detailed information about the meshes considered in this work. The parameter y+ (dimensionless wall distance) should be checked out to establish if the mesh resolution is correct for the applied turbulence model in simulations. In the present case, the y+ values are in agreement with the allowed values set out in ANSYS-CFX® (2009) for the k-ω SST model. Max. Angle and Min. Angle are mesh quality parameters, and they are also in agreement with ANSYS-CFX® (2009). The velocity presented on the table is the velocity in the center of the exit of the test section, and it is showed for convergence analysis. The residual target of the results presented was set up as 10⁻⁶.

Mesh 3 was used in final computations.

Table 1. Mesh size results dependence (3000 rpm).

| Mesh | Nodes | Refinement factor | Max. y+ | Max. Angle | Min. Angle | Velocity (No Screens - m/s) | Time (min) | Velocity (With Screens - m/s) | Time (min) |
|------|---------|-------------------|---------|------------|------------|-----------------------------|------------|-------------------------------|------------|
| 1 | 31052 | - | 8 | 136 | 66 | 8.52 | 3.9 | 8.38 | 3 |
| 2 | 732081 | 23.6 | 5 | 149 | 62 | 8.49 | 36 | 8.25 | 34.7 |
| 3 | 1297708 | 1.8 | 0.94 | 143 | 63 | 8.49 | 204 | 8.25 | 199 |

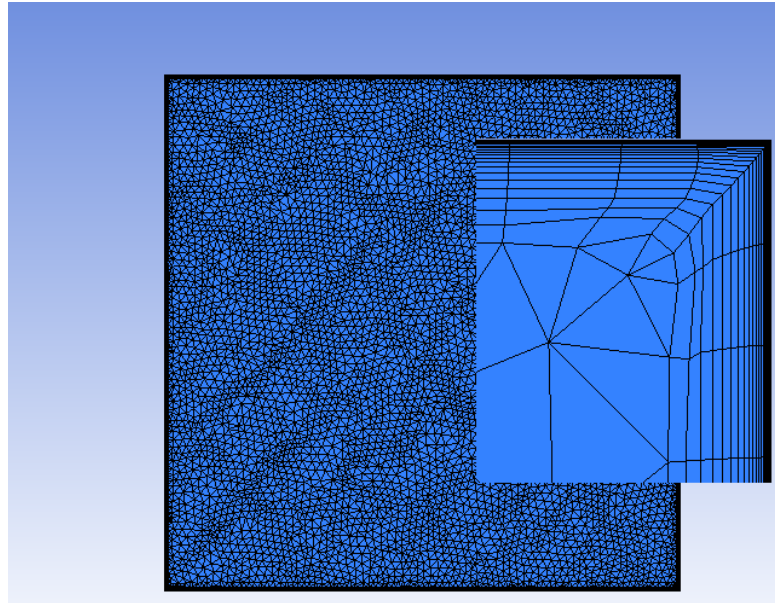


Figure 3: Cross-sectional structure of the computational mesh 1

The axial (z direction) air pressure distribution in the middle line of the test section is shown in Fig. 4 for 3000 rpm for wind tunnel fitted with three and no screen between diffusers. As expected the pressure decreases towards the outlet region of the tunnel, following almost a linear distribution of the pressure drop. It can be seen that this kind of flow presents very small pressure gradients. It was evaluated the pressure drop considering a fully developed flow inside the test section. The pressure drop obtained by numerical simulation for 3000 rpm for wind tunnel fitted with three and no screen between diffusers was 3.86 Pa e 4.06 respectively, showing a percentage difference of 4.91 % in the inlet. The value obtained considering a fully developed flow Eq. (8) was 2.36 Pa and 2.50 Pa for wind tunnel fitted with three and no screen between diffusers respectively. According to Guzella (2010) the discrepancy between the results can be explained due to the assumption of the fully developed flow in the analytical solution.

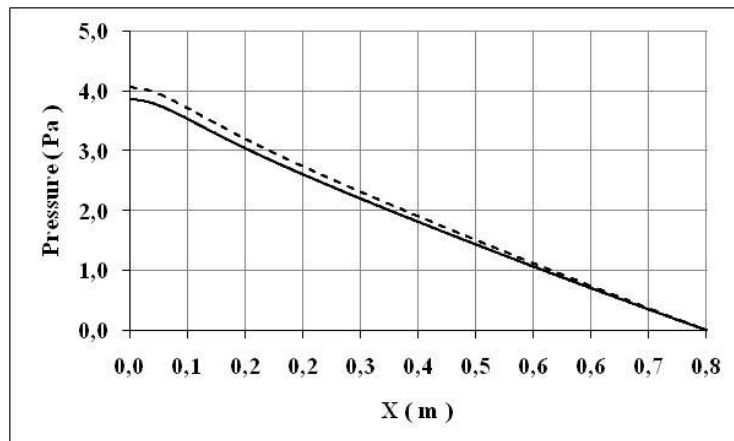


Figure 4: Axial relative pressure distribution along the middle line of the test section, for the wind tunnel fitted with three and no screen between diffusers

The turbulent kinetic energy numerical profiles for mesh 3 in the center of the exit region for the wind tunnel fitted with three and no screen between diffusers are displayed in Fig. 5. We observed higher values of turbulent kinetic energy for the assembly of the tunnel without screens between diffusers. These profiles are compared with an experimental value $0.05746 \text{ m}^2/\text{s}^2$ and $0.07807 \text{ m}^2/\text{s}^2$ for the wind tunnel fitted with three and no screen between diffusers obtained in the center of the tunnel using a hot wire anemometer sensor (Soares, 2008).

The turbulent kinetic energy is associated with the rms velocity fluctuations. Laufer (1948) showed, using a hot wire anemometer that the rms fluctuations in a turbulent developed channel flow are smaller in the regions near the walls and have a sharp maximum near the edges of the laminar sub layers; present a strong movement of kinetic energy

away from these points. The behavior of the turbulent kinetic energy of the numerical simulations is very similar to that described by Laufer (1948) for a channel flow.

Future works should address more refined experiments in near wall regions to perform a more complete analysis. At the mean time the model predicts well the turbulent kinetic energy in the central region of the tunnel in comparison with the available experimental data.

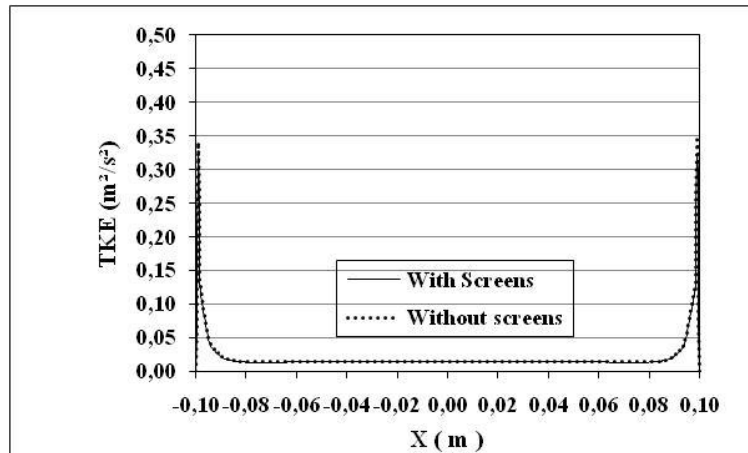


Figure 5: Turbulent kinetic energy for the wind tunnel fitted with three and no screen between diffusers

A comparison of velocity profiles is shown in Fig 6. The average velocities obtained experimentally was 7.86 m / s and the simulations indicated an average speed of 8.25 m / s, a percentage difference of 4.728%. Comparing with the experimental data, the major differences are observed in the regions near the tunnel walls, especially in the left side. This behavior can be explained to small distortions of the wood wind tunnel walls; which produce an asymmetry of the experimental velocity profiles.

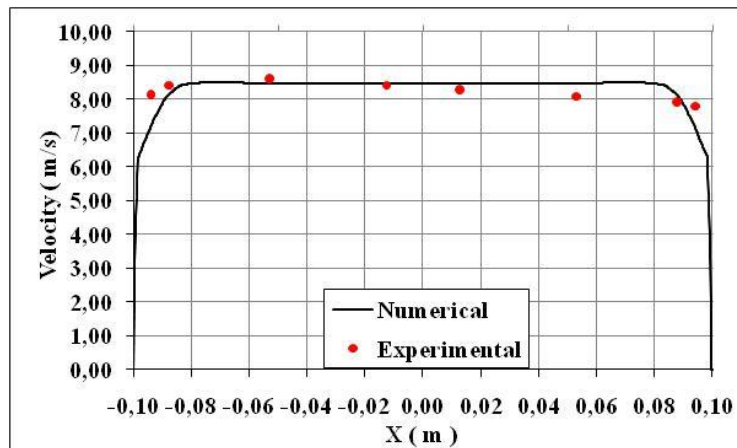


Figure 6: Velocity profiles at the exit wind tunnel section for fitted with three screens between diffusers

In Fig. 7 is shown a comparison of the velocity profiles at the exit wind tunnel section fitted without screens between diffusers. The average velocities obtained experimentally was 8.09 m / s and the simulations indicated an average speed of 8.49 m / s, a percentage difference of 4.71%. Comparing with the experimental data, the major differences as quoted are observed in the regions near the tunnel walls, especially in the left side.

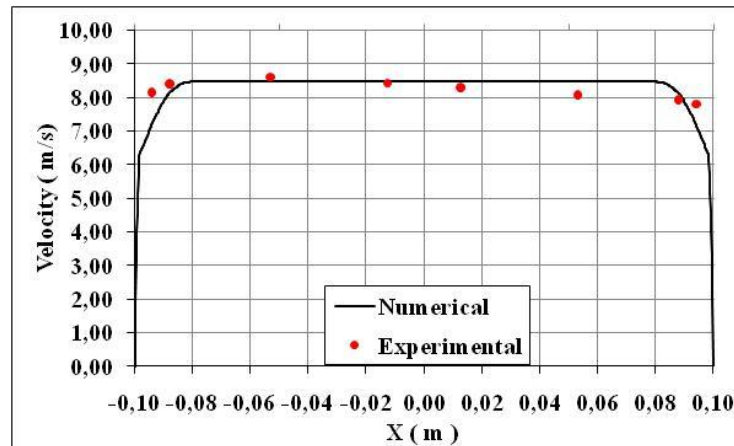


Figure 7: Velocity profiles at the exit wind tunnel section for fitted without screens between diffusers

In Fig. 8 shows a comparison of the instantaneous velocities $U(t)$, obtained in tests of thermal anemometry (HWA), with the tunnel fitted with three and no screen between the diffusers, for the blower frequency of 3000 rpm, data acquisition elapsed time of 20 seconds, however the data presented are from a time of 0.05 s. In tests with HWA mean velocities and turbulent intensities obtained experimentally were 8.14 m/s and 2.49% for the wind tunnel with three screens mounted between diffusers and 8.23 m/s and 2.82% for the tunnel without the screen.

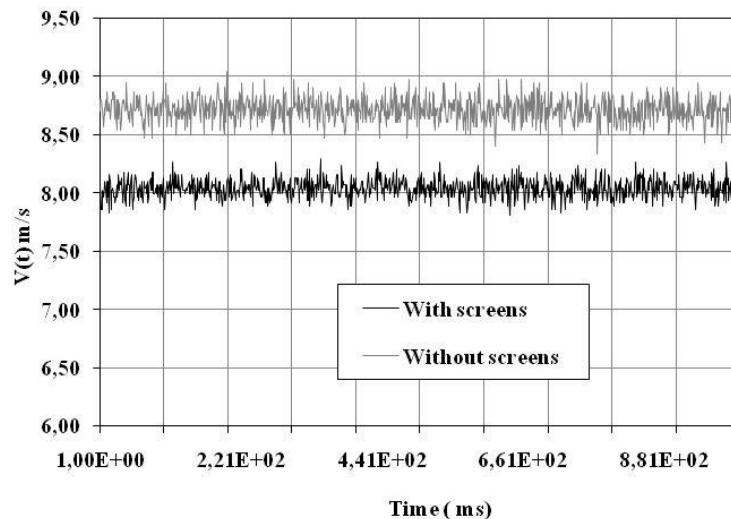


Figure 8: $U(t)$ blower driven at 3000 rpm for the wind tunnel fitted with three and no screen between diffusers

4. CONCLUSIONS

This paper presents a comparison between numerical and experimental data in the test section of a wood low speed open wind tunnel. Experiments with Pitot tube and hot wire anemometry measurements were made to examine the flow behavior in the exit region of the wind tunnel. Numerical results were obtained using the $k-\omega$ SST turbulence model. The simulation results were compared with the mean time experimental cross-section velocity profiles as a function of one value of the inlet mass flow rate, as well as with the experimental value of the turbulent kinetic energy in the centre of the exit region of the wind tunnel. The numerical velocity profile was also compared with a solution for a hydrodynamic fully developed turbulent channel flow. The pressure drop along the test section obtained numerically was confronted with literature correlation. The comparison of the numerical results with experimental data and with the fully developed solution showed that the employed mathematical model produced reasonable results.

5. ACKNOWLEDGEMENTS

Authors are grateful to, Federal Center of Technological Education of Minas Gerais (CEFET-MG) and Pontifical Catholic University of Minas Gerais (PUC Minas), who supports this work.

6. REFERENCES

- ANSYS-CFX® Solver Theory manual, Release 12.1, 2009.
- ASTM INTERNATIONAL DESIGNATION D 3464, 2007 – “Standard Test Method for Average Velocity in a Duct Using a Thermal Anemometer”.
- Baker C.J.; 2007. “Wind engineering— past, present and future”. *Journal of Wind Engineering and Industrial Aerodynamics*. v. 95 843–870
- Carregari, A. L., 2006. “Estudo do Escoamento de Ar Sobre a Carroceria de um Ônibus Usando um Programa de CFD e Comparação com Dados Experimentais”. Dissertação de Mestrado em Engenharia Mecânica – Programa de Pós Graduação da Escola de Engenharia de São Carlos, Universidade de São Paulo, São Carlos, São Paulo, 110f.
- Queiroz, M. D, Souza G. G. A., Soares C. B., Hanriot S. M., Cabezas-Gómez L., Maia C. B., 2009. “Evaluation of Turbulence Models on the Behavior of the Airflow in the Test Section of an Open Low Speed Wind Tunnel”. *Proceedings of the 8TH Brazilian Conference on Dynamics Control and Applications*. São Paulo, Brazil.
- Guzella, M.S.; Manto D.; Soares, C.B.; Maia, C. B.; Hanriot, S. M.; Cabezas-Gómez, L.; 2010. “ Airflow CFD Modelling in the Test Section of a Low-Speed Wind Tunnel.” *Journal of Advanced Research in Mechanical Engineering (JARME)*. v.1, p. 210-225.
- INTERNATIONAL ORGANIZATION for STANDARDIZATION. ISO 3966:2008 Second Edition; 2008; “Measurements of fluid flow in closed conduits- Velocity area method using Pitot static tubes”.
- Jenni-Eiermann, S., Hasselquist, D., Lindström, Å., Koolhaas, A. , Piersma, T. ,2009. “Are birds stressed during long-term flights? A wind-tunnel study on circulating corticosterone in the red knot.” – *General and Comparative Endocrinology*, Volume 164, Issues 2-3, Pages 101-106.
- Kandaa, I., Ueharaa, K., Yamaoa, Y., Yoshikawab, Y., Morikawab, T., 2006. “A wind-tunnel study on exhaust gas dispersion from road vehicles—Part I: Velocity and concentration fields behind single vehicles” - *Journal of Wind Engineering and Industrial Aerodynamics*.
- Kandaa, I., Ueharaa, K., Yamaoa, Y., Yoshikawab, Y., Morikawab, T., 2006. “A wind-tunnel study on exhaust-gas dispersion from road vehicles”—Part II: Effect of vehicle queues - *Journal of Wind Engineering and Industrial Aerodynamics*.
- Kim, J.H.; Ahn, J.W., Kim, C.; Kim, Y.; Chi, K.W., 2006. “Construction of Numerical Wind Tunnel on the e-science Infrastructure, *Proceedings of Parallel Computational Fluid Dynamics*”. Busan, Korea. pp. 99-106.
- Laufer, John ,1948. “Investigation of turbulent flow in a two-dimensional channel”. PhD Thesis. California Institute of Pasadena.
- Liu, X., Levitan, M., Nikitopoulos, D.,2008. “Wind tunnel tests for mean and drag and lift coefficients on multiple circular cylinders arranged in-line” - *Journal of Wind Engineering and Industrial Aerodynamics*.
- Liu, X.P., Niu, J.L., Kwok, K.C.S., Wang, J.H., Li, B.Z., 2010. “Investigation of indoor air pollutant dispersion and cross-contamination around a typical high-rise residential building: wind tunnel tests”. *Journal of Building and Environment*, Volume 45, Issue 8, Pages 1769-1778.
- Malalasekera W.; Versteeg H. K., 1995. “An Introduction to Computation Fluid Dynamics The Finite Volume Method”. Longman Group Ltd. First Published.
- Metha R.D e P. Bradshaw;1979. “Design Rules for Small Low Speed Wind Tunnels”. *The Aeronautical Journal of the Royal Aeronautical Society* .
- Moonen, Peter *et al.*, 2006. “Numerical modeling of the flow conditions in a closed-circuit low-speed wind tunnel”. *Journal of Wind Engineering and Industrial Aerodynamics*, v.94, p.699-723.
- Quim, N., 2007. “Desenvolvimento de uma Metodologia de Simulação Aplicada ao Sistema de Arrefecimento Veicular”. Dissertação de Mestrado em Engenharia Mecânica – Programa de Pós Graduação da Escola Politécnica da Universidade de São Paulo, São Paulo. 140 f.
- Soares, C. B., 2008. “Experimental Study of the Velocity Profiles in Test Section of an Open Low Speed Wind Tunnel”. 138f. Master Degree Dissertation, Pontifical Catholic University of Minas Gerais, Belo Horizonte, Brazil.
- Soares, C. B.; Maia, C. B.; Cabezas-Gómez L.; Hanriot S. M.; 2009. “Numerical and Experimental Evaluation of the Velocity Profiles in Test Section of an Open Low Speed Wind Tunnel”. *7 th Word Conference on Experimental Heat Transfer , Fluid Mechanics and Thermodynamics*.
- Winkler J.; Temel F.Z; Carolus T.; 2007. “Concept, Design and Characterization of a Small Aeroacoustic Wind Tunnel Facility With Application To Fan Blade Measurements”. *Fan Noise*. p.1-12.

7. RESPONSIBILITY NOTICE

The authors are the only responsible for the printed material included in this paper.